THE JOURNAL OF PHYSICAL CHEMISTRY C

Article

pubs.acs.org/JPCC

Electropolymerization: Further Insight into the Formation of Conducting Polyindole Thin Films

Balázs B. Berkes,*[,†,‡] Aliaksandr S. Bandarenka,*[,§,∥] and György Inzelt[†]

[†]Department of Physical Chemistry, Institute of Chemistry, Eötvös Loránd University, H-1117 Budapest, Pázmány Péter sétány 1/A, Hungary

[‡]Battery and Electrochemistry Laboratory, Institute of Nanotechnology, Karlsruhe Institute of Technology, Hermann-von-Helmholtz-Platz 1, 76344 Eggenstein-Leopoldshafen, Germany

[§]Nanosystems Initiative Munich (NIM), Schellingstrasse 4, 80799 Munich, Germany

[∥]Physik-Department ECS, Technische Universität München, James-Franck-Strasse 1, 85748 Garching, Germany

Supporting Information

ABSTRACT: Electropolymerization is a promising route to design new functional surfaces. In this work, we investigate electropolymerization of indole at polycrystalline Pt electrode surfaces in acidic sulfuric media using in situ nanogravimetry, electrochemical impedance spectroscopy, and direct current (dc) measurements applied simultaneously to elucidate the physical model of the electrified interface during this process. Monitoring the electrode mass change with a quartz crystal nanobalance allows quantification of the overall electropolymerization kinetics and, together with the dc-response, provides further insight into the dynamics of the film formation. Complementary electrochemical impedance spectroscopy measurements quantify specific parameters characterizing the processes which involve the interfacial charge transfer during the film growth. Importantly for various applications, it has been also demonstrated that the growth of polyindole thin films can be controlled using just molecular oxygen dissolved in the electrolytes.

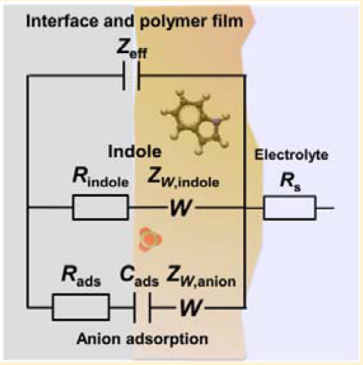

1. INTRODUCTION

Electrochemically controlled formation of thin polymer films at electrode surfaces is one of the viable routes to design new functional materials. Application areas of thus synthesized coatings range from corrosion protection of metals, through electrochromic devices, to state of the art means of energy conversion and storage.[1] The properties of the resultant polymer films can be very different depending on the nature of precursors, electrolyte composition, and the electrochemical conditions of their synthesis. Therefore, deeper understanding of electropolymerization is of particular importance to further advance technological processes and to design new functional coatings.

Notably, modern physicochemical and specific electrochemical approaches to gain deeper understanding of functionality of polymer films are commonly based on characterization of those coatings, which are already *preformed* on the electrode surface in essentially inert electrolyte media; relatively less is known about the status of the electrode/electrolyte interface during the formation of polymer coatings. [We need to notice that the most accepted definition of an electrode is that it is the *half-cell* between one electron conductor and at least one ionic conductor (see e.g., ref 2). In our case the electron conductor phase, however, changes during the electrode process. The role of the metal will be displaced partially or completely by the forming polymer layer. Therefore, in order to avoid misunderstandings, in this work we will consequently describe the interface between the electron and ionic conductor as the electrode/electrolyte interface, remarking that the electrode in this sense does not match the most accepted concept.] Nevertheless, the conditions and mechanisms of electropolymerization normally determine the properties of the resulting materials. Moreover, while electrochemical polymerization is a promising route to form coatings with defined properties, the choice of organic precursors is still relatively limited. The origin of this situation is largely determined by our current understanding of various phenomena taking place at the electrode surface during this kind of processes. While a qualitative description of electrochemical reactions at the electrode surfaces is in many cases known, a detailed in situ characterization of dynamic interfacial changes during electropolymerization is often very difficult. However, it is the electrified solid/liquid interface which largely determines the film properties.

In this work, we target a better understanding of the electrochemically assisted formation of polyindole polymer films (in acid electrolytes), which is suggested to be among the promising functional conducting polymer materials.[2−6] One of the main advantages of the system is that indole can be easily electropolymerized in a well-controllable manner at relatively low positive electrode potentials. Furthermore, it is one of the

Received: December 8, 2014
Published: January 7, 2015

DOI: 10.1021/jp512208s
J. Phys. Chem. C 2015, 119, 1996−2003

good examples of systems where both the adsorption and electrodeposition play an important role determining the status of the electrified interface. However, the polyindole film formation is less studied despite this conducting polymer having many promising applications.

For in situ characterization of the polyindole film growth, we have utilized complementary direct current (dc), electrochemical impedance spectroscopy (EIS), and nanogravimetric measurements. While polymerization of indole has already been carried out,[7−11] in this work we conduct the first study which involves simultaneous dc, EIS, and electrochemical quartz crystal nanobalance (EQCN) measurements to describe the mechanism of the electropolymerization processes of indole. It should be stressed again that we aim at multiparametric characterization of the growing film, not already preformed coatings. The complementary EIS-EQCN experiments help in forming a physical model of the electrode/electrolyte interface and give the overall and local kinetic information about this process.[12,13] Importantly for possible application needs, it is also demonstrated that the growth of polyindole thin films at the Pt surface can be controlled using just molecular oxygen dissolved in the electrolyte.

2. EXPERIMENTAL SECTION

Analytical grade chemicals such as H_2SO_4, $HClO_4$ (Merck), and indole (Sigma-Aldrich) were used as received. Doubly distilled water was utilized (Millipore water). The solutions of indole were always freshly prepared. The solutions were deaerated before the monomer was dissolved. To enhance the dissolution process, an ultrasonic bath was used. All solutions were purged with oxygen-free argon (purity: 5.0, Linde Gas Hungary Co. Cltd.), and an inert gas blanket was maintained throughout the experiments.

AT-cut crystals (5 MHz) of 1-in. diameter coated with platinum having a titanium underlayer (Stanford Research Systems, SRS, Sunnyvale, CA) were used in the EQCN measurements. The electrochemically and the piezoelectrically active areas were equal to 1.37 cm^2 and 0.4 cm^2, respectively. The integral sensitivity of the crystals (C_f) was found to be 56.6 $\times$ 10^6 Hz g^{-1} cm^2, i.e., 1 Hz corresponds to 17.7 ng cm^{-2}. A Pt wire was used as a counter electrode. The reference electrode was a sodium chloride saturated calomel electrode (SCE) with a double frit. All of the potentials is this work are given with the reference to a SCE scale. A Biologic VSP potentiostat was used for the measurements.

The electrochemical cell was cleaned before the measurements by leaving it overnight in a $KMnO_4$ solution and afterward rinsed with a solution of diluted sulfuric acid and hydrogen peroxide and then boiled in doubly distilled water for several hours while changing the water at least two to three times. The crystal holder was cleaned with a "piranha" solution.

The concentration of the monomer solutions was 1 mmol dm^{-3}. Polymerization was carried out either by potentiodynamic cycling in a 1 mol dm^{-3} $HClO_4$ solution at a scan rate of 10 mV s^{-1} or at a constant potential in sulfuric acid media (0.1 mol dm^{-3} H_2SO_4) in order to elucidate the influence of the anion specific adsorption. The applied potential ranges/potentials are indicated at the discussion of the experiments. The cycling of the potential as a pretreatment of the electrode was carried out before each experiment in the supporting electrolyte, until a stable voltammogram characteristic for a clean Pt surface[14] was obtained.

Impedance measurements were carried out in the frequency range 1 Hz to 30 kHz with an amplitude of 5 mV (V_{rms} ≈ 3.54 mV) while the potential was kept constant at 0.7 V vs SCE. Ten frequency points were measured per decade, logarithmically equally distributed (45 points per spectrum). The saved spectra were representative for at least four measurements.

The EIS spectra analysis, including Kramers−Kronig tests, was performed with the EIS Spectrum Analyzer software,[15] and the quality of the model validation was determined as described elsewhere.[16] Further information on the quality and reliability of fitting is available in the Supporting Information.

3. RESULTS AND DISCUSSION

3.1. Voltammetric and Nanogravimetric Measurements. Figure 1 shows a sequence of typical cyclic voltammograms (CVs) characterizing electrochemically assisted polymerization of indole at polycrystalline Pt electrodes. A series of growing anodic and cathodic waves in the voltammograms commonly reveals the complexity of the processes taking place during the electrochemical formation of polyindole (PI),[17,18] even for CVs taken in perchlorate electrolytes without concurrent adsorption of anions such as ClO_4^-. Nevertheless, according to the literature data, the anodic waves at the potentials more positive than ∼0.53 V likely correspond to the formation of new active polymerization centers at the electrode surface.[19] A series of quasisymmetrical peaks between ∼0.0 V and ∼0.53 V correspond to the following transformations in the resulting polymer film as shown in Scheme 1. However, a more detailed analysis of the electropolymerization using only voltammetric data is complicated as several processes can contribute simultaneously to the measured direct current.

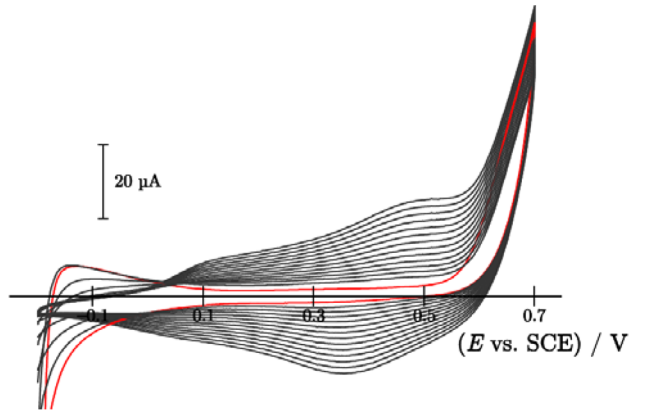

Figure 1. Cyclic voltammograms acquired during the polymerization of indole in 40 consecutive cycles, scan rate: 10 mV s^{-1}. For the sake of better visibility, only every 3rd cycle is shown. First cycle is shown by the red line. c_{indole} = 1 mmol dm^{-3} in 1 mol dm^{-3} $HClO_4$.

Scheme 1. Proposed Mechanism of Redox Transformations at the Electrode Surface during Electropolymerization of Indole, Where X^- Designates Anions in an Electrolyte

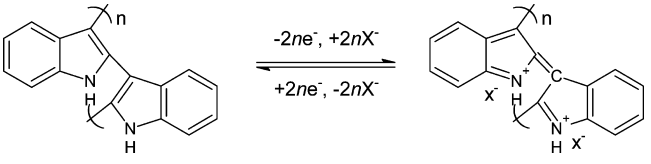

DOI: 10.1021/jp512208s
J. Phys. Chem. C 2015, 119, 1996−2003

It is possible to extract additional information about the polymer growth mechanism if the direct current measurements are complemented with simultaneous monitoring of the electrode mass changes with EQCN. For that, the electrode potential was fixed in the region, where both the generation of new active polymerization centers as well as new phase growth are possible (0.7 V). Figure 2 shows the results of this

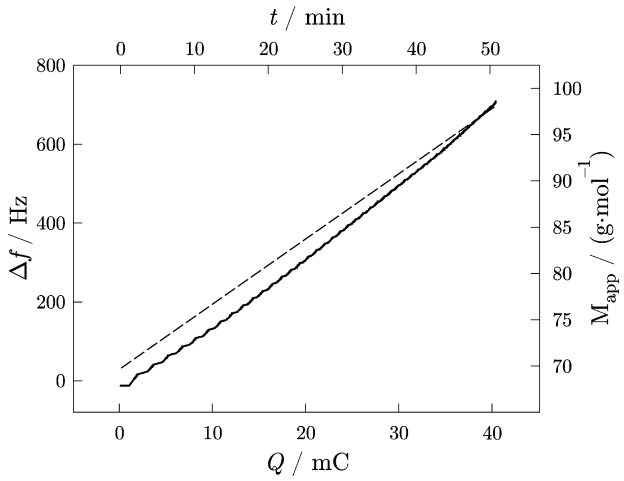

Figure 2. Frequency change (Δf) during the deposition of polyindole at 0.7 V in 0.1 mol dm^{-3} H_2SO_4 as a function of time (t) and charge (Q) (solid line). The charge was calculated from the current measured during the potentiostatic deposition. The dashed line shows the change of the apparent molar mass with time calculated from the Δf vs Q curve, assuming one-electron interfacial transfer.

experiment, illustrating how the total charge, Q, the resonance frequency (which is proportional to the electrode mass), Δf, and the apparent molar mass of the electroactive species, M_{app}, change with time.

Figure 2 gives information about the overall kinetics of electrochemically assisted polymerization via the analysis of the total electrode mass change as a function of time. It can be seen from the figure that electrodeposition of the polymer film proceeds steadily at this potential with a noticeable "self-propagation" or "acceleration" of the process. Further analysis of the dependence of Q on Δf (Figure 2) helps to estimate the apparent molar mass of electroactive species contributing to the direct current and EQCN response. Interestingly, M_{app} significantly changes with time. Assuming mechanisms involving only one interfacial electron transfer per one indole molecule, M_{app} should be close to ~117 g/mol. However, experimental values vary between ~70 and ~100 g/mol. This can be explained by the fact that initial stages of the polymer formation involve certain local overoxidation of the growing polymer,[20,21] e.g., resulting in the following fragments (PI_{over}):

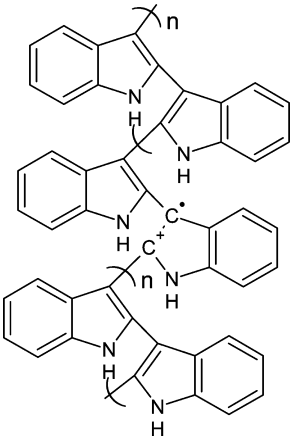

This increases substantially the number of electrons which should be accounted for in the overall balance. Additionally, adsorption/desorption of *O and *OH from H_2O at the Pt

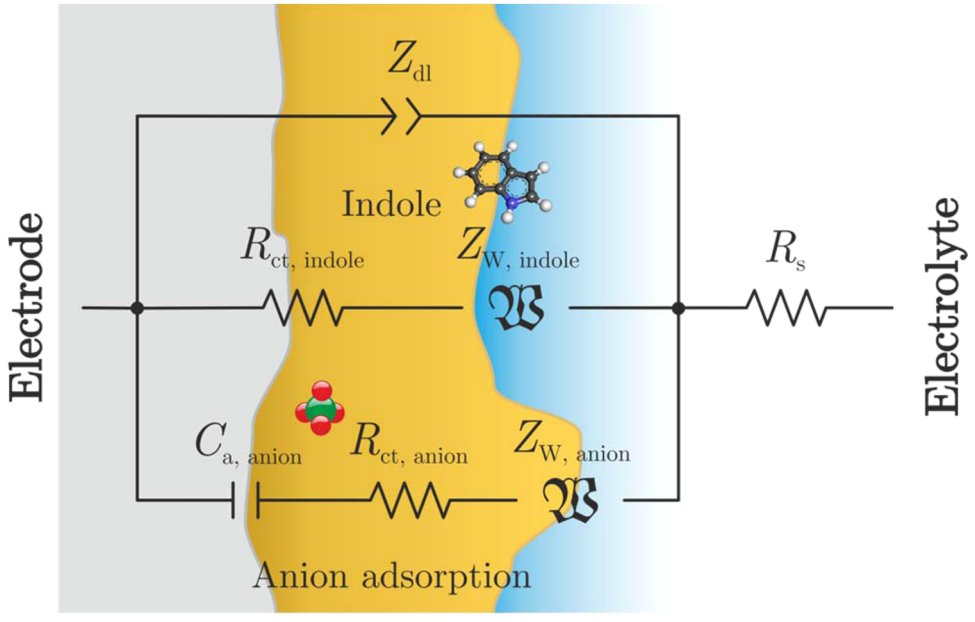

Figure 3. Equivalent electric circuit describing the EIS response of polyindole deposition on platinum. Z_{dl} represents the impedance of the double layer, $R_{ct,indole}$ and $Z_{W,indole}$ are the charge transfer and diffusional impedances of indole, respectively, $C_{a,anion}$ is the capacitive impedance related to the counterion adsorption (on Pt surface), $R_{ct,anion}$ is the charge transfer resistance associated with the counterion adsorption/desorption, $Z_{W,anion}$ is the diffusional impedance of the counterions, and R_s is the solution resistance.

DOI: 10.1021/jp512208s
J. Phys. Chem. C 2015, 119, 1996−2003

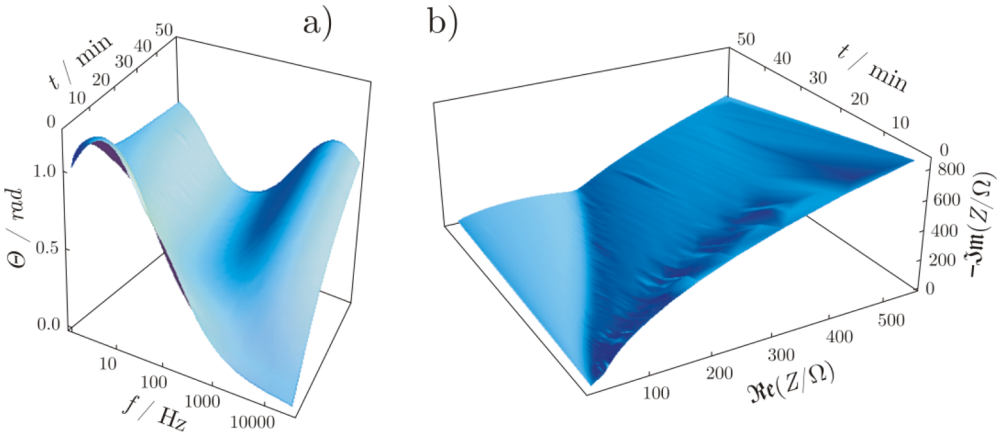

Figure 4. Three-dimensional representation of the (A) Bode and (B) Nyquist plots of the measured impedance data during the electrodeposition of indole at 0.7 V in 0.1 mol dm^{-3} H_2SO_4 solution.

surface or other background processes can contribute to this effect.

3.2. Analysis of EIS Data. According to the Dolin–Ershler–Randles approximation, the EIS response of the electrode/electrolyte interface normally contains capacitive contributions originating from the interfacial impedance, Z_{dl}, and from processes which involve the charge transfer through it (so-called Faradaic processes, with the overall impedance Z_F); the latter can be considered as a sort of "leakage" of the interfacial "capacitance". Using a three-electrode measurement scheme, one should additionally take into account the response of the ionically conducting electrolyte, Z_s, to carefully describe the impedance spectra. In the case of ionically conducting liquid electrolytes, it can be approximated with a resistance, i.e., $Z_s = R_s$.

The exact description of the other two constituents of the EIS response also depends on the properties of electrochemical interface as well as on the modeling approach. In the following, we will use an approach involving a so-called equivalent electric circuit (EEC) which can in many cases be considered as a graphical representation of mathematical equations describing the electrochemical system.

Figure 3 presents the equivalent electric circuit which has been elucidated based on a priori chemical knowledge about this system. The interfacial impedance, Z_{dl}, can be in general case described using a semiempirical constant phase element (CPE), $Z_{dl} = C'^{-1}_{dl}(j\omega)^{-\varphi}$. In this formula C'_{dl} is the parameter directly proportional to the interfacial capacitance, exponent φ with typical values $1 \leq \varphi \leq 0.75$ takes into account possible frequency dispersion (for the cases when $\varphi < 1$), j is the imaginary unit, and ω is angular frequency.

In order to elucidate an expression for the Faradaic impedance, Z_F, it is important to assume that at least two parallel processes involving the interfacial charge transfer are possible during the polyindole film growth: (i) anodic activation of indole molecules and (ii) adsorption/desorption of anions (e.g., SO_4^{2-} and HSO_4^- anions). Under small-amplitude EIS probing, only the Faradaic current, due to anodic oxidation ($i_{F,indole}$), and surface concentrations ($c_{s,indole}$) of the electroactive species oscillate around quasi-steady-state values. (We assume that the surface concentration of the monomer will play the decisive role.) A linear part of the response can be written as

$$\Delta i_{F,indole} = \left(\frac{\partial i_{F,indole}}{\partial E}\right)\Delta E + \left(\frac{\partial i_{F,indole}}{\partial c_S}\right)\Delta c_{S,indole} \quad (1)$$

where Δ corresponds to the parameters which periodically oscillate during the probing. Similarly, in the case of specific anion adsorption and desorption, the corresponding Faradaic current ($i_{F,anion}$), surface concentrations of the anions ($c_{s,anion}$), and, additionally (due to highly reversible nature of the adsorption), their fractional surface coverages (θ_{anion}) will oscillate periodically. A linear part of the response can be accordingly written as

$$\Delta i_{F,anion} = \left(\frac{\partial i_{F,anion}}{\partial E}\right)\Delta E + \left(\frac{\partial i_{F,anion}}{\partial \theta_{anion}}\right)\Delta\theta_{anion} + \left(\frac{\partial i_{F,anion}}{\partial c_{S,anion}}\right)\Delta c_{S,anion} \quad (2)$$

Solving eqs 1 and 2 and considering that according to the Dolin–Ershler–Randles approximation the total impedance Z_{tot}:

$$Z_{tot} = Z_s + (Z_{dl}^{-1} + Z_{F,indole}^{-1} + Z_{F,anion}^{-1})^{-1}$$

the following expression for the overall impedance can be written:

$$Z_{tot} = R_s + \left((j\omega)^{\varphi} C'_{dl} + \frac{1}{R_{ct,anion} + (j\omega C_{a,anion})^{-1} + Z_{D,anion}} + \frac{1}{R_{ct,indole} + Z_{D,indole}}\right)^{-1} \quad (3)$$

where $R_{ct,anion} = -1/(\partial i_{F,anion}/\partial E)$, $R_{ct,indole} = -1/(\partial i_{F,indole}/\partial E)$ are the interfacial charge transfer resistances for the adsorption of anions and indole, respectively, $C_a = -q_{anion}(\partial\theta_{anion}/\partial E)$ is the anion adsorption capacitance, q_{anion} is the charge necessary to form a complete adsorbate layer of anions, $Z_{D,indole}$, $Z_{D,anions}$ are diffusion impedances, which are usually represented by the corresponding Warburg impedances, $Z_{W,indole} = A_{W,indole}(j\omega)^{-0.5}$ and $Z_{W,anion} = A_{W,anion}(j\omega)^{-0.5}$, and $A_{W,indole}$ and $A_{W,anion}$ are the Warburg coefficients, respectively.

DOI: 10.1021/jp512208s
J. Phys. Chem. C 2015, 119, 1996–2003

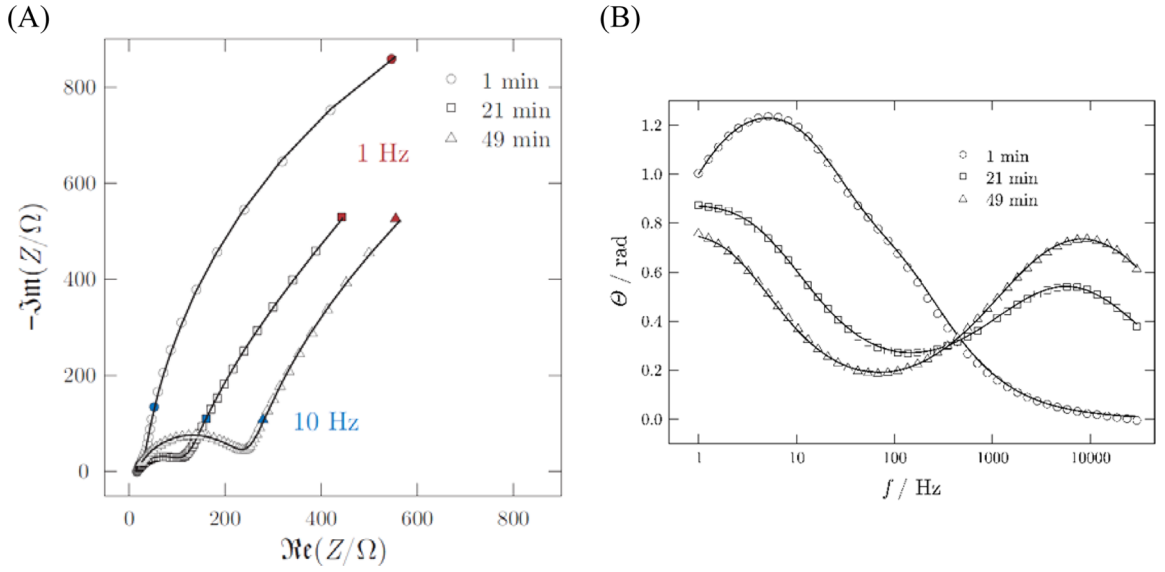

Figure 5. Results of the fitting (solid lines) together with experimental data at different stages of the deposition of polyindole films. (A) Nyquist plots; (B) Bode plots.

Equation 3 can be graphically represented by the equivalent circuit shown in Figure 3. The parameters of eq 3 can be used to monitor the status of the electrified interface during the electropolymerization process.

It can be assumed that the Faradaic current due to indole anodic activation is a complex function of time and the electrode potential:

$$I_{F,indole} \propto A_{sc}(t, E)c_{s,indole}(t, E)k_{app,indole}(t, E)f(R_{\Omega}, ...)$$

where the function $A_{sc}(t,E)$ corresponds to the changing "active" surface area of the electrode with time, which can be considered as a scaling geometrical factor, the function $c_{s,indole}(t,E)$ is the surface concentration of electroactive monomer or protonated indole species, the function $f(R_{\Omega},...)$ accounts for other possible contributions such as changes in the film resistance, etc., and the apparent rate coefficient of the anodic process $k_{app,indole}(t,E)$ is, in turn, a complex function of the local rate coefficients. Therefore, taking into account two parameters, $R_{ct,indole}$ and $A_{W,indole}$, available from EIS fitting procedure, it is possible to monitor changes in $k_{app,indole}(t,E)$ as a function of time:

$$\frac{A_{W,indole}(t, E)}{R_{ct,indole}(t, E)} = k_{app,indole}(t, E)(\sqrt{2D_{indole}})^{-1} \quad (4)$$

Similarly, it is possible to monitor anion adsorption/desorption kinetics:

$$\frac{A_{W,anion}(t, E)}{R_{ct,anion}(t, E)} = k_{app,anion}(t, E)(\sqrt{2D_{anion}})^{-1} \quad (5)$$

Figure 4 shows experimental impedance data in 3D extended Bode (Figure 4A, phase shift as a function of frequency and time) and Nyquist (Figure 4B, imaginary part of impedance as a function of the real part and time) representations. From Figure 4, it is evident that components of the impedance response drastically depend on time and therefore can reveal information about stages related to electrochemical activation of the indole polymerization process.

Figure 5 presents typical examples of fitting the experimental impedance data to the model presented in Figure 3 (see also Supporting Information showing more detailed fitting results of all impedance spectra obtained in this work). As shown in Figure 5, experimental data fit well to the EEC, with acceptably small individual parameter errors, thus verifying the model.

Figures 6−8 present the parameters of the model shown in Figure 3 as a function of time that give further information about the polymer formation process. Figure 6A,B gives an overview of how the inverse charge transfer resistance and

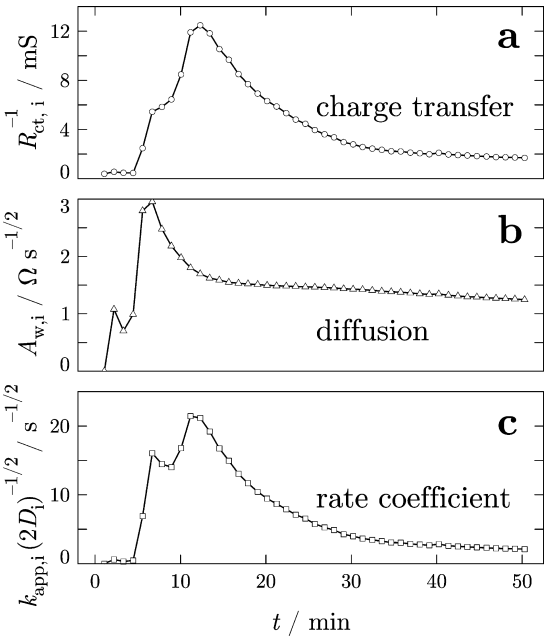

Figure 6. Changes of the indole-related parameters of the model presented in Figure 3. (A) The inverse charge transfer associated with indole, $R_{ct,i}$. (B) The corresponding Warburg coefficient $A_{W,i}$. (C) The kinetic parameter characterizing the relative contribution of "fast" and "slow" deposition events involving the interfacial charge transfer, $k_{app,i}(2D_i)^{-0.5}$. The parameters are normalized (per cm^{-2}).

DOI: 10.1021/jp512208s
J. Phys. Chem. C 2015, 119, 1996−2003

Warburg coefficient associated with indole itself vary with time, providing evidence that after an inductive period, the process of generation of active centers is at its maximum, contributing to noticeable diffusion limitations. Figure 6C summarizes essential information from Figure 6A,B: it shows how the kinetic parameter $k_{app,indole}(2D_{indole})^{-0.5}$ related to the interfacial charge transfer (see eq 4) changes during the process. The dependence of the apparent rate coefficient presented in the figure mainly reflects the relative contribution of slow and fast electrochemical stages involving the interfacial charge transfer during the film growth.[22] In general, formation of nuclei of a new phase is considerably slower than their growth. Assuming that the diffusion coefficient is approximately constant during the deposition process, one can see from Figure 6C that during the first ~5 min the contribution of the relatively slow charge transfer events dominates, as expected, taking into account that the nuclei (initial formation of active polymerization centers) of polyindole should be initially formed at the Pt surface. After ~5 min, the contribution of the faster interfacial charge transfer events becomes significant. This is revealed by the peak between ~5 min and ~20 min in Figure 6C. As a first approximation, we hypothesize that the fast events can mainly include the formation of new active polymerization centers at the Pt/PI(nuclei) boundary as well as the formation of the overoxidized fragments. After ~20 min, $k_{app,indole}(2D_{indole})^{-0.5}$ decreases significantly and remains approximately constant, suggesting that the relative contribution of the slower stages is increased. This behavior is to a certain extent expected, taking into account that the surface of Pt is covered by the polymer film, so that the growth at the Pt/PI boundary is suppressed. However, one can also expect that the diffusion coefficient of the indole molecules in/at the relatively thick indole film is decreased, contributing to the corresponding decrease of the $k_{app,indole}(2D_{indole})^{-0.5}$ parameter.

As mentioned above, sulfate anions contribute to the ac response, particularly due to their reversible adsorption/desorption at the Pt surface. It is possible to monitor the dynamics of SO_4^{2-}/HSO_4^- adsorption during the film growth through the dependencies of the respective EEC parameters as a function of time. Figure 7A shows such dependence for the adsorption capacitance of the anions. At a given potential, this parameter is directly proportional to the fraction of the adsorbate at the surface which "oscillates" during the ac probing ($C_a = -q_{anion}(\partial\theta_{anion}/\partial E)$). In other words, the adsorption capacitance does not directly depend on the total surface coverage but rather reveals the fraction of the adsorbate which reversibly adsorbs and desorbs during the measurements at a certain potential. As one can see from Figure 7A, the sulfate adsorption capacitance significantly changes during the polymer film growth. At the anodic potential selected for polymerization, it is known that the sulfate surface coverage is ~0.2 monolayer (ML) in H_2SO_4, and the adsorption capacitance is approximately a few μF cm^{-2}, as the adsorbate layer is almost "saturated".[12] Figure 7A shows that after 5 min of indole electropolymerization, the adsorption capacitance increases up to ~200 μFcm^{-2}. This value roughly corresponds to 0.1 ML of sulfates adsorbing and desorbing during the low-amplitude ac probing, i.e., ~50% of the available adsorbed sulfates are "disturbed" during initial stages of polymerization. However, after ~10 min, the adsorption capacitance decreases (~100 μF cm^{-2}) and remains approximately constant. The nonzero values of the adsorption capacitance after ~10 min indirectly suggest that redox transformations at the polymer/Pt interface still

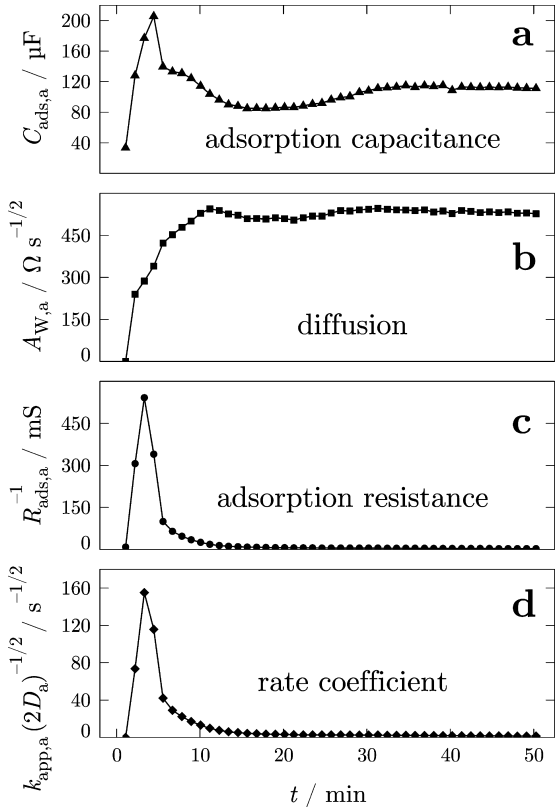

Figure 7. Dependencies of the EEC parameters related to sulfate adsorption which accompanies polyindole film deposition. $C_{ads,a}$ and $R_{ads,a}$ are the adsorption-related capacitances and resistances of (bi)sulfate anions, $A_{W,a}$ is the Warburg coefficient, $k_{app,a}$ is the apparent rate coefficient of adsorption which characterizes adsorption at the surface partly covered with the adsorbate, and D_a is the diffusion coefficient of (bi)sulfate anions. The parameters are normalized (per cm^{-2}).

significantly disturb the adsorbed sulfate layer. However, the kinetics of this adsorption process is diminished as can be observed using other relevant EEC parameter dependencies (Figure 7B–D), mainly the adsorption resistance, Warburg coefficient, and the apparent rate coefficient.

Perhaps the most difficult parameter dependencies to interpret are those related to the constant phase element, which is used to model the behavior of the double electric layer. As has been recently demonstrated, the lower exponent values correspond to various situations when the double electric layer does not respond to the ac probing as an ideal capacitance (see, e.g., refs 23 and 24 and references therein). Moreover, the so-called ideal capacitive behavior does not necessarily correspond to the expected structures and phenomena at the surface.[23,25−28] For example, the disorder/order phase transitions and other structuring processes at the electrode surface largely contribute to the CPE behavior of solid electrodes, while common expectations would rather suggest the opposite. Particularly, formation of the ordered sulfate structures decrease the CPE exponent, likely due to the fact that the ordering at the interface causes dissipation of the energy of the probing signal.[23,28]

As can be seen from Figure 8, just before the polymerization is initiated, the CPE exponent is rather low, being less than 0.9. This is consistent with the data presented recently for the similar system. Surprisingly, the exponent grows to ~1.0 after

DOI: 10.1021/jp512208s
J. Phys. Chem. C 2015, 119, 1996−2003

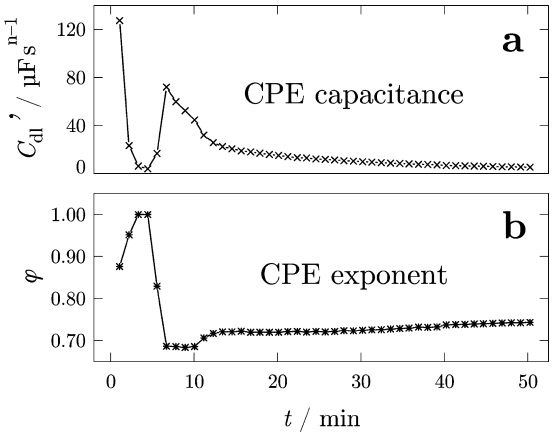

Figure 8. Time dependencies of the parameters related to the impedance of the double layer. C'_{dl} is a parameter of the CPE which is directly proportional to the double layer capacitance ("CPE capacitance"), and φ is the exponent in the CPE.

approximately 3 min of the polymerization process. This is somehow against the common expectation that the ideal capacitive behavior of the double layer is the prerequisite of an "undisturbed system". However, this is in line with the hypothesis of Kolb and Pajkossy,[26] who suggested that the CPE behavior is in many cases due to the structuring effects at the interface. Taking this hypothesis into account, one can qualitatively explain the dependencies in Figure 8 at least within the experimental time before ~8 min. The polymerization process largely disturbs the ordered sulfate structures at the surface, causing the CPE exponent to grow. However, after ~8 min, the exponent drops to ~0.75. Without particular interpretation, it reveals that the interface itself largely dissipates the energy of the probing signal. This is not surprising, as the latter comprises the rigid polymer film at the interface which likely cannot respond ideally to the ac perturbation.

In connection with the polymerization of indole, the adsorption of the monomer was also studied. Figure 9 shows the results of an experiment in which the frequency and potential change of a platinum EQCN electrode was monitored. For the sake of clarity, the immersion-related frequency change and the initially established stable frequency and potential responses in the deaereted solution are not shown in the figure.

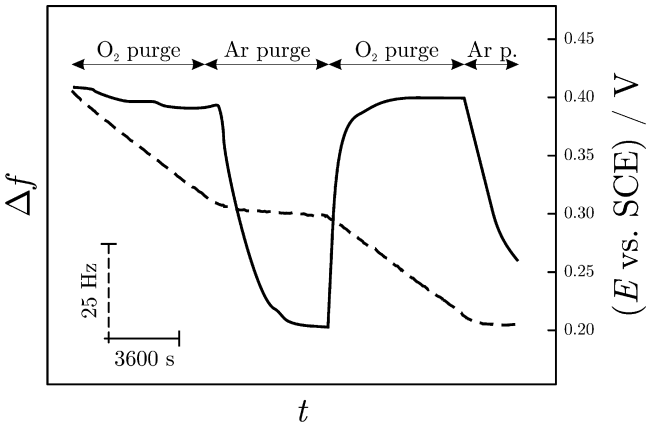

Figure 9. Part of a frequency change curve (dashed line) and a curve showing the change of the open circuit potential (solid line) obtained for a Pt EQCN electrode from an experiment where the 1 mmol dm^{-3} indole-containing electrolyte was purged with air and argon repeatedly. Electrolyte: 0.1 mol dm^{-3} H_2SO_4.

Purging oxygen into the monomer-containing solution results in a continuous frequency decrease. The rate of the change remains approximately constant for relatively long times (for hours) and the same for the two sections when oxygen was bubbled. This rate (i.e., the slope of the $\Delta f(t)$ curve) is ≈14 Hz h^{-1}.

Deoxygenating the solution with high purity argon gradually stops the decrease of the frequency. Both the potential and the frequency reach a steady-state value. The potential stabilizes at 0.2 V. The stabilization is relatively long in time, and it requires the complete removal of oxygen, since even traces of oxygen in the solution induce the deposition of the monomer. This reveals abrupt changes when purging the solution with oxygen again. The deposition occurs with the same rate as in the previous section. The ability to generate conducting polymers on a platinum surface in this simple, however controlled, way, even without the use of a potentiostat, may open new vistas in the production of polymer-modified electrodes.

4. CONCLUSIONS

In this work, we for the first time used complementary dc, EIS, and EQCN techniques to provide further insight into the process of electropolymerization of indole on Pt electrodes. The use of these techniques revealed a significant amount of overoxidized species and polymer fragments during the film growth. This has been evident from the electrochemical nanogravimetry data which were analyzed simultaneously with dc current data. Analysis of EIS data further simplifies elucidation of the physical model of the electrode/electrolyte interface, which can be expressed as the equivalent electric circuit. Using this model, it is possible to separate the capacitive behavior of the electrified interface itself, the contribution of the Faradaic process due to the monomer activation and polymer fragments (over)oxidation, and the Faradaic contribution of the inorganic anions which adsorb/desorb at the Pt electrode surface. Furthermore, by monitoring the time dependencies of the parameters of the model, it is possible to detect changes of the film growth modes. Finally, EQCN measurements appeared to be indispensable tool to monitor the formation of the polyindole film which can be initiated and controlled by the oxygen molecules dissolved in the electrolyte. The latter process can likely be used to form polyindole thin films without the use of potentiostats or equivalent electrochemical (electrical) devices.

■ ASSOCIATED CONTENT

Supporting Information

More detailed fitting results of all impedance spectra obtained in this work. This material is available free of charge via the Internet at http://pubs.acs.org.

■ AUTHOR INFORMATION

Corresponding Authors

*E-mail: balazs.berkes@kit.edu.
*E-mail: bandarenka@ph.tum.de.

Notes

The authors declare no competing financial interest.

DOI: 10.1021/jp512208s
J. Phys. Chem. C 2015, 119, 1996−2003

■ ACKNOWLEDGMENTS

A.S.B. acknowledges financial support from SFB 749, the cluster of excellence Nanosystems Initiative Munich (NIM). Financial support of the National Scientific Research Fund (OTKA K100149) (G.I.) is gratefully acknowledged.

■ REFERENCES

(1) Inzelt, G. Conducting Polymers: A New Era in Electrochemistry. *Monographs in electrochemistry*; Springer: New York, 2012.
(2) Cai, Z.; Yang, G. Synthesis of Polyindole and Its Evaluation for Li-Ion Battery Applications. *Synth. Met.* **2010**, *160*, 1902−1905.
(3) Maarouf, E. B.; Billaud, D.; Hannecart, E. Electrochemical Cycling and Electrochromic Properties of Polyindole. *Mater. Res. Bull.* **1994**, *29*, 637−643.
(4) Moretti, G.; Quartarone, G.; Tassan, A.; Zingales, A. 5-Amino- and 5-Chloro-Indole as Mild Steel Corrosion Inhibitors in 1 N Sulphuric Acid. *Electrochim. Acta* **1996**, *41*, 1971−1980.
(5) Pandey, P. C. Copper (II) Ion Sensor Based on Electropolymerized Undoped-Polyindole Modified Electrode. *Sens. Actuators, B* **1999**, *54*, 210−214.
(6) Xu, J.; Hou, J.; Zhou, W.; Nie, G.; Pu, S.; Zhang, S. ^{1}H NMR Spectral Studies on the Polymerization Mechanism of Indole and Its Derivatives. *Spectrochim. Acta, Part A* **2006**, *63*, 723−728.
(7) Berkes, B. B.; Inzelt, G. Electrochemical Nanogravimetric Studies on the Electropolymerization of Indole and on Polyindole. *Electrochim. Acta* **2014**, *122*, 11−15.
(8) Billaud, D.; Maarouf, E. B.; Hannecart, E. Chemical Oxidation and Polymerization of Indole. *Synth. Met.* **1995**, *69*, 571−572.
(9) Holze, R.; Hamann, C. H. Electrosynthetic Aspects of Anodic Reactions of Anilines and Indoles. *Tetrahedron* **1991**, *47*, 737−746.
(10) Pandey, P. C.; Prakash, R. Electrochemical Synthesis of Polyindole and Its Evaluation for Rechargeable Battery Applications. *J. Electrochem. Soc.* **1998**, *145*, 999−1003.
(11) Tourillon, G.; Garnier, F. New Electrochemically Generated Organic Conducting Polymers. *J. Electroanal. Chem.* **1982**, *135*, 173−178.
(12) Berkes, B. B.; Inzelt, G.; Schuhmann, W.; Bondarenko, A. S. Influence of Cs^{+} and Na^{+} on Specific Adsorption of *OH, *O, and *H at Platinum in Acidic Sulfuric Media. *J. Phys. Chem. C* **2012**, *116*, 10995−11003.
(13) Berkes, B. B.; Maljusch, A.; Schuhmann, W.; Bondarenko, A. S. Simultaneous Acquisition of Impedance and Gravimetric Data in a Cyclic Potential Scan for the Characterization of Nonstationary Electrode/Electrolyte Interfaces. *J. Phys. Chem. C* **2011**, *115*, 9122−9130.
(14) Berkes, B. B.; Inzelt, G. Generation and Electrochemical Nanogravimetric Response of the Third Anodic Hydrogen Peak on a Platinum Electrode in Sulfuric Acid Media. *J. Solid State Electrochem.* **2014**, *18*, 1239−1249.
(15) Bondarenko, A. S.; Ragoisha, G. A. Inverse Problem in Potentiodynamic Electrochemical Impedance. In *Progress in Chemometrics Research*; Pomerantsev, A. L., Ed., Nova Science Publishers: New York, 2005; pp 89−102.
(16) Bondarenko, A. S. Analysis of Large Experimental Datasets in Electrochemical Impedance Spectroscopy. *Anal. Chim. Acta* **2012**, *743*, 41−50.
(17) Billaud, D.; Maarouf, E. B.; Hannecart, E. Electrochemical Polymerization of Indole. *Polymer* **1994**, *35*, 2010−2011.
(18) Talbi, H.; Monard, G.; Loos, M.; Billaud, D. Theoretical Study of Indole Polymerization. *J. Mol. Struct.: THEOCHEM* **1998**, *434*, 129−134.
(19) Saraji, M.; Bagheri, A. Electropolymerization of Indole and Study of Electrochemical Behavior of the Polymer in Aqueous Solutions. *Synth. Met.* **1998**, *98*, 57−63.
(20) Berkes, B. B.; Nemes, Á.; Moore, C. E.; Szabó, F.; Inzelt, G. Electrochemical Nanogravimetric Study of the Electropolymerization of 6-Aminoindole and the Redox Transformations of the Polymer Formed in Aqueous Media. *J. Solid State Electrochem.* **2013**, *17*, 3067−3074.
(21) Berkes, B. B.; Inzelt, G.; Vass, E. Electrochemical Nanogravimetric Study of the Adsorption of 4-Aminoindole and the Surface Layer Formed by Electrooxidation in Aqueous Acid Media. *Electrochim. Acta* **2013**, *96*, 51−60.
(22) Berkes, B. B.; Henry, J. B.; Huang, M.; Bondarenko, A. S. Electrochemical Characterisation of Copper Thin-Film Formation on Polycrystalline Platinum. *ChemPhysChem* **2012**, *13*, 3210−3217.
(23) Tymoczko, J.; Schuhmann, W.; Bandarenka, A. S. The Constant Phase Element Reveals 2D Phase Transitions in Adsorbate Layers at the Electrode/Electrolyte Interfaces. *Electrochem. Commun.* **2013**, *27*, 42−45.
(24) Bandarenka, A. S. Exploring the Interfaces between Metal Electrodes and Aqueous Electrolytes with Electrochemical Impedance Spectroscopy. *Analyst* **2013**, *138*, 5540−5554.
(25) Pajkossy, T. Impedance of Rough Capacitive Electrodes. *J. Electroanal. Chem.* **1994**, *364*, 111−125.
(26) Pajkossy, T.; Kolb, D. M. Anion-Adsorption-Related Frequency-Dependent Double Layer Capacitance of the Platinum-Group Metals in the Double Layer Region. *Electrochim. Acta* **2008**, *53*, 7403−7409.
(27) Motheo, A. J.; Sadkowski, A.; Neves, R. S. Electrochemical Immittance Spectroscopy Applied to the Study of the Single Crystal Gold/Aqueous Perchloric Acid Interface. *J. Electroanal. Chem.* **1997**, *430*, 253−262.
(28) Tymoczko, J.; Colic, V.; Bandarenka, A. S.; Schuhmann, W. Detection of 2D Phase Transitions at the Electrode/Electrolyte Interface Using Electrochemical Impedance Spectroscopy. *Surf. Sci.* **2015**, *631*, 81−87.

DOI: 10.1021/jp512208s
J. Phys. Chem. C 2015, 119, 1996−2003